Comparison with an uncertainty of 2×10^{-16} between two primary frequency standards

Cipriana Mandache, C. Vian, P. Rosenbusch, H. Marion,
Ph. Laurent, G. Santarelli, S. Bize and A. Clairon
LNE-SYRTE, Observatoire de Paris
Paris, France
e-mail: cipriana.mandache@obspm.fr

A.N. Luiten, M.E. Tobar
University of Western Australia
Crawley, AUSTRALIA

C. Salomon
Laboratoire Kastler Brossel, Ecole Normale Supérieure,
Paris, France

Abstract— **We present a comparison between SYRTE's Cs fountain FO1 and Cs-Rb fountain FO2 using a cryogenic sapphire oscillator (CSO) to generate an ultra-stable interrogation signal. A description of the experimental setup is given and the clock accuracies are discussed. For the first time, a frequency resolution in the low 10^{-16} is achieved in the comparison between two primary standards. The paper also summarizes recent contributions of these fountains to research activities such as test of the stability of fundamental constants, timekeeping and test of sub-systems of the PHARAO space clock.**

I.   INTRODUCTION

Over the years, SYRTE has developed three atomic fountain clocks: FO1 using Cs atoms, FO2 which can operate with either Cs and Rb atoms, and FOM a transportable Cs fountain. FO1 and FO2 have recently undergone substantial changes and are currently operated using a cryogenic sapphire oscillator as the basis for the synthesis of the interrogation signals. One of these two clocks has shown short term fractional frequency instability of $1.6\times10^{-14}\,\tau^{-1/2}$.

In this paper, we first briefly describe the fountains developed at SYRTE. We then discuss the systematic shifts that affect the accuracy of these fountains. We give an evaluation of the size of these shifts and of the accuracy to which they are determined. We then describe a direct frequency comparison between FO1 and FO2 fountains with a fractional frequency uncertainty of 2 parts in 10^{16} at 50000 seconds. We finally mention the use of these fountains for testing the stability of fundamental constants and for other applications.

II.   SYRTE FOUNTAINS

A first Cs fountain FO1, in operation since 1994 [1] has been recently refurbished and improved. A second Cs fountain FOM is a transportable fountain derived from the PHARAO space clock prototype [2]. The third fountain FO2 is a dual fountain operating with Cs or Rb in the same apparatus. It is described in [3]. In the following, we briefly outline the present design of these fountains and theirs recent improvements.

A schematic of the fountain, making explicit the arrangement for the dual Cs-Rb fountain is shown in Fig. 1. All three fountains now operate with lin ⊥ lin optical molasses. For FO1, the molasses is loaded from a laser slowed atomic beam, leading to a typical capture rate of 3.10^8 atoms in 400ms. For FO2, an additional transverse cooling of the atomic beam increases this rate to 10^9 atoms in 300ms. For FOM, a vapor cell optical molasses is used. After loading, atoms are launched upwards at ~4 m.s⁻¹ using the moving optical molasses technique and cooled to ~1μK.

State selection is accomplished through appropriate manipulation of the atomic cloud by means of a selection microwave cavity and a push laser beam, as shown in Fig.3. Further details concerning the state selection process will be given in the following.

About 50 cm above the capture zone, a cylindrical copper cavity (TE_{011} mode) is used to probe the hyperfine transition in a Ramsey interrogation scheme. The cavities have a loaded quality factor of Q_{FO1} = 10 000, Q_{FO2} = 6600 (Cs cavity). Cavities can be fed through two coupling irises oppositely located on the cavity diameter. The microwave radiations that feed the cavities are synthesized from the output of an ultra-stable cryogenic sapphire resonator oscillator (CSO) developed at the University of Western Australia [4]. This cryogenic oscillator has fractional frequency instability below 1×10^{-15} between 1s and 800s averaging times.

Detection of atoms after the interrogation phase is accomplished by laser induced fluorescence. A signal to noise ratio of ~ 5000 per shot is obtained in the measurement of the transition probability.
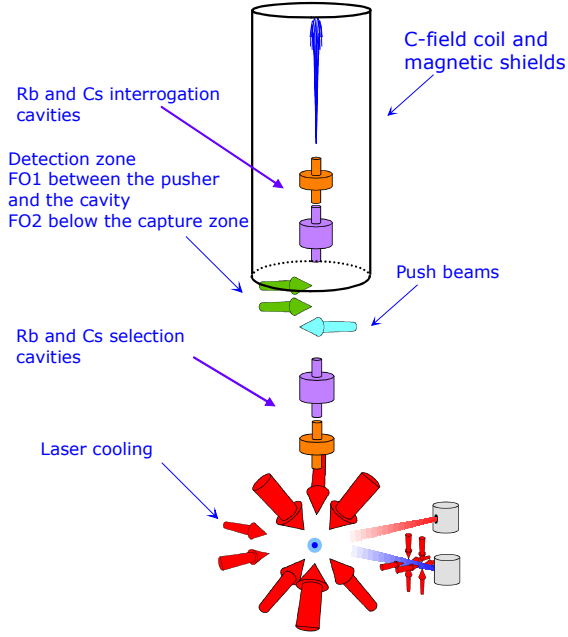
Figure 1: Schematic of an atomic fountain.

III. FREQUENCY STABILITY

Fig.2 shows the fractional frequency instability of FO1 and FO2 against the cryogenic sapphire oscillator as a function of averaging time τ. For averaging times above the servo-loop time constant (~3s) and below 100s, the fractional frequency instability is equal to $2.9 \times 10^{-14} \tau^{-1/2}$ for FO1 and $1.6 \times 10^{-14} \tau^{-1/2}$ for FO2. These are the best stabilities reported to date for primary frequency standards.
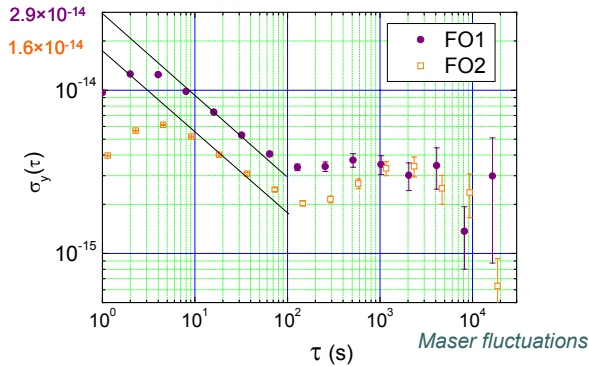

Figure 2: Fractional frequency instability of FO1 and FO2 against the cryogenic sapphire oscillator.

For averaging times above 100s, the frequency instability is dominated by the frequency fluctuations of the CSO weakly phase-locked to a hydrogen maser.

The achievement of such stabilities is a crucial step for studying and evaluating of systematic shifts at the 10^{-16} level.

IV. SYSTEMATIC FREQUENCY SHIFTS IN FO1, FO2 AND FOM

The Table I shows the accuracy budget of FO1, FO2 and FOM fountains. The comparison that will be described in the following fully confirms the accuracies mentioned in this table.

TABLE I: Systematic frequency shifts for FO1, FO2 (during the comparison described in the following (paragraph VI)) and FOM

	$(\times 10^{-16})$ FO1	$(\times 10^{-16})$ FO2	$(\times 10^{-16})$ FOM
Quadratic Zeeman effect	1199.7 ± 4.5	1927.3 ± 0.3	351.9 ± 2.4
Blackbody radiation	-162.8 ± 2.5	-168.2 ± 2.5	-191.0 ± 2.5
Cold collisions and cavity pulling	-197.9 ± 2.4	-357.5 ± 2.0	-34.0 ± 5.8
Microwave spectral purity & leakage	< 3.3	<4.3	0.0 ± 2.4
1st order Doppler effect	<3	<3	<2
Ramsey et Rabi pulling	<1	<1	<1
Microwave recoil	<1.4	<1.4	<1.4
2nd order Doppler effect	<0.08	<0.08	<0.08
Background collisions	<1	<1	<1
Total uncertainty	± 7.5	± 6.5	± 7.7

A. Cold collision

In order to control and to reduce the cold collision shift, we have proposed and demonstrated a new method based on adiabatic population transfer [5]. This method allows the preparation of atomic samples with well defined density ratio. In this method, the initial selection of the F=3, m_F=0 clock state is done by sweeping the selection microwave frequency across the atomic resonance. Two configurations are used:

1. Full adiabatic population transfer, leading to the selection of 100% of the F=4,m_F=0 atoms (high density, HD),
2. Interrupted adiabatic population transfer where the microwave interaction is interrupted when the detuning goes to zero, leading to the selection of only 50% of the F=4,m_F=0 atoms (low density, LD).

The advantages of this method are its insensitivity to experimental imperfections (distribution of the field amplitude in the selection cavity, microwave power fluctuations) and the absence of any significant modification of the velocity distribution and position. The combination of these two advantages allows for a precise measurement of the cold collision shift and an extrapolation to zero density with a fractional uncertainty of few parts in 10^3.

In practice the clock is operated alternatively in HD for 60 s and in LD for 60 s. This timing choice minimizes the noise due to frequency instability of the CSO oscillator. The cold collision shift is deduced from the frequency difference

between HD and LD data. Typically, this measurement is done with a statistical uncertainty of 10^{-16} in one day. In addition, the numbers of detected atoms in F=3 and F=4 are stored and analyzed for both configurations. The ratios of the detected atom numbers between the LD and the HD configurations are computed for both F=3 and F=4 states. Fig.3 shows the stability of this ratio as a function of the cycle number. Both ratios average down as white noise below 10^{-3}. For FO1 the measured ratios are:

$$\frac{N_{F=4}^{50\%}}{N_{F=4}^{100\%}} = \frac{1}{2}(1 + (2 \pm 0.2) \times 10^{-3})$$

$$\frac{N_{F=3}^{50\%}}{N_{F=3}^{100\%}} = \frac{1}{2}(1 + (6 \pm 0.2) \times 10^{-3})$$

The deviation from ½ of these ratios is accounted for in the calculation of the uncertainty due to the cold collision shift. For F=3 we see a slightly larger deviation from ½ due to spurious populations in F=3, $m_F \neq 0$ states in the initial cloud.
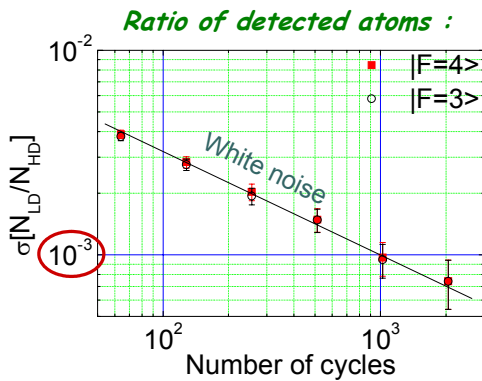

Figure 3: Instability of the ratio of the detected atom number between LD and HD configurations as a function of the number of fountain cycles. Each cycle lasts 1.3s. The instability decreases as the square root of the number of cycles.

Note that this measurement method also accounts for the cavity frequency pulling [6] which is also proportional to the number of launched atoms.

B. Quadratic Zeeman effect

In the past, the uncertainty related to the quadratic Zeeman effect was a significant contribution due to the relatively high by magnetic field fluctuations of the Paris urban environment. Recently, very significant improvements in the control of this effect have been achieved. A key ingredient has been to fine-tune the gains of the various coils used to actively stabilize the magnetic field in the fountain. The static magnetic field is monitored every 10 minutes using the F=3,m_F=1 => F=4,m_F=1 transition, leading to a control of the magnetic field to +/- 0.02nT for FO2. For FO1, fine-tuning of the active servo-loop has not been implemented leading to the higher corresponding

uncertainty in Tab. I. Fig. 4 represents the measurement of the bias magnetic field in the interrogation region of FO2 as a function of time. Fig. 5 shows a map of magnetic field in the FO2. The magnetic field is homogeneous to +/- 2×10^{-3}.
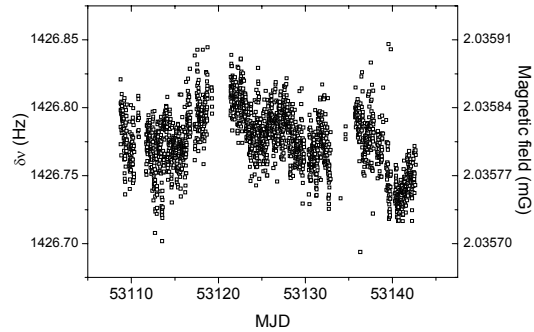

Figure 4: Measurement of the bias magnetic field in the interrogation region of the FO2 fountain.
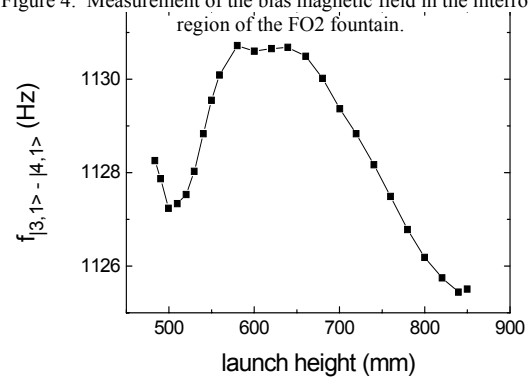

Figure 5: Map of magnetic field in the FO2 fountain. The magnetic field is measured in term of the frequency of the F=3,m_F=1 => F=4,m_F=1 transition with a sensitivity of 700.84 Hz.mG^{-1}.

C. Distributed cavity phase shift

A frequency shift due to the first order Doppler effect can occur if the microwave field inside the interrogation cavity has a phase gradient and the atoms cross the cavity with a slight inclination with respect to gravity. Both in FO1 and FO2, the interrogation cavity is fed using two oppositely located feedthroughs in order to cancel the main term in the phase distribution. We determine the frequency shift due to this main component by measuring the clock frequency when coupling the microwave interrogation signal either 'from the left' or 'from the right' or symmetrically into the cavity. Using atoms as a probe, it is possible to control the field inside the cavity both in phase and amplitude to better than ~1%, and balance the two feeds at this level. Additionally, repeated measurements show that this adjustment is stable at the 1% level over a few weeks. For FO2, the observed shift between the 'left' and symmetric configuration is $(-25.3 \pm 1.1) \times 10^{-16}$ while the shift

between the 'right' and symmetric configuration is $(+24.0\pm1.2)\times10^{-16}$. Given the good coupling symmetry measured in FO2, we estimate that the symmetric feed cancel this effect to better than 5%. At this level, the second order term in the phase distribution becomes the limiting factor. Based on the prediction of Schröder [7] and Gibble [8] concerning the quadratic term, numerical computation indicates that the corresponding shift doesn't exceed 3×10^{-16}.

For FO1, the effect of the feed-related phase gradient is found to be 5 times smaller, due to a higher cavity quality factor and a better alignment of the launch direction. Despite a larger asymmetry between the couplings, we estimated that symmetric feeding reduces the effect of the feed-related component below the quadratic term.

Measurements of the distributed cavity phase shift are currently being performed in FO2. These measurements should allow an interesting comparison with some aspects of the model developed by Gibble [8].

D. Blackbody radiation shift

The blackbody radiation shift is evaluated based of the Stark shift measurement of [23]. A 10% uncertainty is attributed to the T^6 term [24]. In FO2, an ensemble of thermistors monitors continuously the temperature and its gradient. Recent improvements brought the uncertainty on the temperature from $\pm1K$ to $\pm0.2K$. The entire set-up of FO1 is at the laboratory temperature and monitored with an uncertainty of $\pm1K$.

E. Effects of microwave spectral purity and leakage

In order to evaluate the effect of microwave spectral purity and leakage in the interrogation region, four measurements are made, at LD and HD for $\pi/2$ pulses, and at LD and HD for $3\pi/2$ pulses (a variation of a factor 9 in microwave power). For both microwave amplitudes, we extrapolate the collision shift, which may also change with the microwave power. Within the resolution of the measurements, no frequency shift is observed. This method does not distinguish between shifts due to synchronous perturbations, microwave leakages and spurious microwave lines. Therefore, the measurement statistical uncertainties of 3.3×10^{-16} for FO1 and 4.3×10^{-16} for FO2 are conservatively taken as the uncertainties due to microwave spectral purity and leakage, with no extrapolation.

V. COMPARISON SETUP

The measurement set-up used for timekeeping and comparisons between atomic fountains is shown in Fig. 6. For the first time we have operated two atomic fountains together with an ultra stable cryogenic sapphire resonator oscillator (CSO) developed at the University of Western Australia. The CSO is weakly phase locked to a hydrogen maser contributing to the local timescale and to TAI (International Atomic Time) through several time and frequency transfer systems. With this setup, atomic fountains are used as primary frequency standard to calibrate TAI and can be compared to other remote clocks.
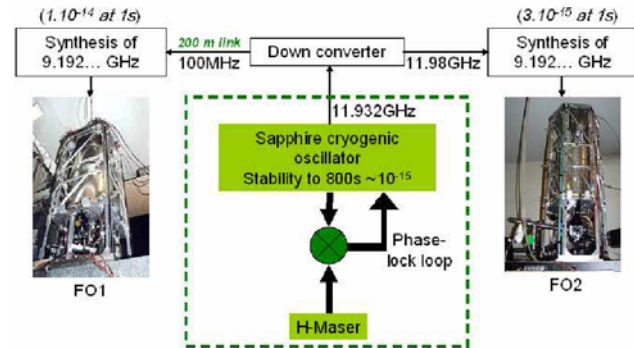

Figure 6: Set-up showing the frequency synthesis and distribution system

The 11.932 GHz output signal from the CSO is converted in order to synthesize 11.98 GHz, 1 GHz and 100 MHz signals, all three being phase-coherent with the H-maser on the long term. FO2 uses the 11.98 GHz signal to generate 9.193 GHz by means of an home-made low noise synthesizer which achieves a frequency instability of 3×10^{-15} at 1 s by operating only in the microwave domain [25]. This scheme reduces at the minimum the phase noise and the spurious side-bands induced by the down conversion process. The 150 m distance between FO1, FOM and the CSO prevents the direct use of the 11.98 GHz signal. Instead, the 100 MHz signal is distributed to FO1 and FOM via a high stability RF cable. Finally, a 100 MHz to 9.193 GHz home-made synthesizer generates the interrogation signal. These additional steps degrade the phase noise of the interrogation signal. Its frequency instability is currently limited to $\sim2\times10^{-14}$ at 1s. Comparisons between fountains are performed by measuring simultaneously the frequency of this common local oscillator (CSO + Maser). To do this, the frequency corrections are time-tagged by NTP protocol referenced to the same local time scale UTC(OP). This scheme allows for the elimination of local oscillator fluctuations in the comparison between the primary frequency standards.

VI. COMPARISON BETWEEN TWO ATOMIC FOUNTAINS USING A CRYOGENIC SAPPHIRE OSCILLATOR

Fig. 7 shows the fractional frequency instability measured between FO1, FO2 and the CSO. Each fountain is operated in differential mode in order to continuously evaluate and cancel the collision shift as explained above.

After all frequency corrections have been made, the FO2 fountain has a frequency stability of 2.8×10^{-14} at 1s, the best reported value to date for a primary frequency standard.
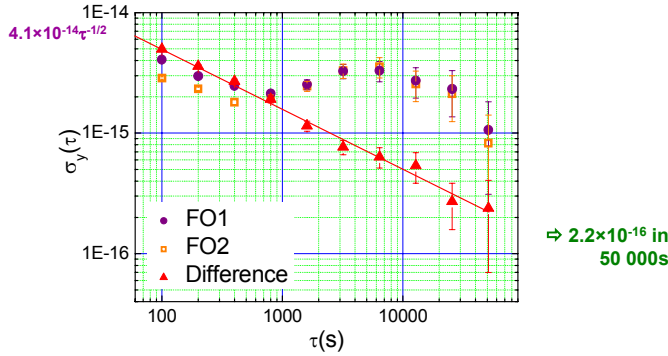
Figure 7: Fractional frequency instability: Squares: FO2 vs CSO, Diamonds: FO1 vs CSO. Triangles: FO2 vs FO1.

Figure 8: Measured ^{87}Rb frequencies referenced to the ^{133}Cs fountains over 72 months.

For averaging times longer than 100s, measurements of each fountain represent the frequency fluctuations of the local oscillator. When analyzing the fractional frequency difference between the two fountain data, we find a combined instability of 5×10^{-14} at 1s. The instability decreases as white frequency noise down to 2.2×10^{-16} at 50000s averaging time. At least one of the two fountains has stability better than 1.6×10^{-16} at the same averaging time. This is the first time that such stability is observed between two primary standards.

The average frequency difference between the two fountains is $(4\pm2.2)\times10^{-16}$. This result is a very strong confirmation of the accuracies stated previously in Table I.

VII. TEST OF THE STABILITY OF FUNDAMENTAL CONSTANTS

Highly accurate atomic clocks offer the possibility of performing laboratory tests of a putative variation of fundamental constants. Fig. 8 summarizes the comparison between ^{87}Rb and ^{133}Cs hyperfine frequencies that has been done at SYRTE using the fountains ensemble described above over duration of 6 years. Each point on the graph summarizes the result of one to two months of measurements which include each time an evaluation of all known systematic effects [12, 13, 14].

A weighted linear fit to the data in Fig. 8 determines how these measurements constrain a possible time variation of ν_{Rb}/ν_{Cs}. We find:

$$\frac{d}{dt}\ln(\frac{\nu_{Rb}}{\nu_{Cs}}) = (-0.5\pm5.3)\times10^{-16}\ yr^{-1}$$

These measurements constraint possible variations of $(g_{Rb}/g_{Cs}\ \alpha^{-0.49})$ at the same level (g_{Cs} ,g_{Rb} nuclear g-factor of Rb and Cs, α fine-structure constant) [22].
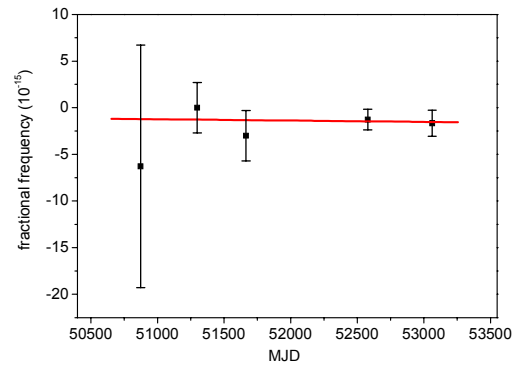
The transportable fountain FOM has similarly been used as a primary standard in the measurement of the frequency ν_H of the hydrogen 1S-2S transition performed at Max-Planck Institute in Garching (Germany) [15,16]. Two measurements performed over a 4 year period constrain fractional variations of ν_{Cs}/ν_H at the level of $(3.2\pm6.3)\times10^{-15}$ yr^{-1}. This limits fractional variations of $g_{Cs}(m_e/m_p)\alpha^{2.83}$ at the same level [9,10]. Combining these results with other recent comparisons (^{199}Hg$^+$ optical clock versus ^{133}Cs fountain [17,18] ^{171}Yb$^+$ optical clock versus ^{133}Cs fountain [19,20]), it is possible to independently set limits to variations of α, g_{Rb}/g_{Cs} and $g_{Cs}(m_e/m_p)$ with time. These measurements test the stability of the electroweak interaction (α) and of the strong interaction (g_{Rb}/g_{Cs}, $g_{Cs}(m_e/m_p)$) separately [16,21] and independently of any cosmological model.

VIII. OTHER RECENT WORK WITH ATOMIC FOUNTAINS

SYRTE atomic fountains also had significant contribution to the following scientific activities:

- TAI calibrations: 13 calibrations have made with FO2 over the past 3 years;
- Remote comparisons with other primary frequency standards (at IEN, NPL, PTB) using GPS and TWSTFT systems;
- Absolute frequency measurements of the Rb hyperfine splitting [13], [22]. The measured value is:

$$\nu_{Rb} = 6\ 834\ 682\ 610.904\ 324(4)(7)\ Hz$$

Following this measurement, the ^{87}Rb hyperfine transition has been recommended by the BIPM CCL/CCTF JWG as a secondary representation of the SI second.

- Test of sub-systems for the PHARAO/ACES cold atom space clock (test of the engineering model of PHARAO microwave synthesizer with FO2, test of the flight model of the PHARAO Ramsey cavity with FO1).

IX. CONCLUSIONS

We performed a direct comparison between two atomic fountains using cryogenic sapphire oscillator as a

local oscillator. We have observed an unprecedented instability of 2.2×10^{-16} at 50 000s between the primary frequency standards FO1 and FO2. In this comparison one of the two standards has shown a short term fractional frequency instability of $2.8 \times 10^{-14} \tau^{-1/2}$. The comparison fully confirms the clock accuracies.

ACKNOWLEDGMENTS

REFERENCES

[1] A. Clairon, et al., A cesium fountain frequency standard: recent results, IEEE Trans. Instrum. Meas. 44 (1995) 128

[2] P. Laurent, et al., A cold atom clock in absence of gravity, Eur. Phys. J. D 3 (1998) 201

[3] Y. Sortais, et al., Cold collision frequency shifts in a 87Rb fountain, Phys. Rev. Lett. 85 (2000) 3117

[4] A.G. Mann, S. Chang, A.N. Luiten, Cryogenic sapphire oscillator with exceptionally high frequency stability, IEEE Trans. Instrum. Meas. 50 (2001) 519.

[5] F. Pereira Dos Santos, et al., Controlling the cold collision shift in high precision atomic interferometry, Phys. Rev. Lett. 89 (2002) 233004.

[6] S. Bize, et al., Cavity frequency pulling in cold atom fountains, IEEE Trans. Instrum. Meas. 50 (2001) 503.

[7] R. Schröder, U. Hübner, D. Griebsch, Design and realization of the microwave cavity in the PTB caesium atomic fountain clock CSF1, IEEE Trans.Ultras.Ferro and Freq.Cont.49, (2002), 383

[8] R. Li, K. Gibble, *Metrologia,* 41 (2004))

[9] J.D. Prestage, R.L. Tjoelker, L. Maleki, Atomic clocks and variations of the fine structure constant, Phys. Rev. Lett. 74 (1995) 3511.

[10] V.A. Dzuba, V.V. Flambaum, J.K. Webb, Calculations of the relativistic effects in many-electron atoms and space–time variation of fundamental constants, Phys. Rev. A 59 (1999) 230.

[11] V.V. Flambaum, D.B. Leinweber, A.W. Thomas, R.D. Young, Limits on the temporal variation of the fine structure constant, quark masses and strong interaction from quasar absorption spectra and atomic clock experiments, Phys. Rev. D 69 (2004) 115006.

[12] H. Marion, et al., Search for variations of fundamental constants using atomic fountain clocks, Phys. Rev. Lett. 90 (2003) 150801.

[13] S. Bize, et al., High-accuracy measurement of the 87Rb ground-tate hyperfine splitting in an atomic fountain, Europhys. Lett. 45 (1999) 558.

[14] S. Bize, et all, Proc. of the 6th Symposium on Frequency Standards and Metrology, (P. Gill ed.), World Scientific, Singapore, 2001, 53

[15] M. Niering, et al., Measurement of the hydrogen 1S–2S transition frequency by phase coherent comparison with a microwave cesium fountain clock, Phys. Rev. Lett. 84 (2000) 5496.

[16] M. Fischer, et al., New limits on the drift of fundamental constants from laboratory measurements, Phys. Rev. Lett. 92 (2004) 230802.

[17] S. Bize, et al., Testing the stability of fundamental constants with the 199Hg+ single-ion optical clock, Phys. Rev. Lett. 90 (2003) 150802

[18] Th. Udem, et al., Absolute frequency measurements of Hg+ and Ca optical clock transitions with a femtosecond laser, Phys. Rev. Lett. 86 (2001) 4996.

[19] E. Peik, et al., New limit on the present temporal variation of the fine structure constant, Physics/0402132, 2004.

[20] J. Stenger, et al., Absolute frequency measurement of the 435.5 nm 171Yb+ clock transition with a Kerr-lens mode-locked femtosecond laser, Opt. Lett. 26, 1589 (2001)

[21] P. Laurent, et al., Cesium fountains and micro-gravity clocks, in: Proc. of the 25th Moriond Conf. on Dark Matter in Cosmology, Clocks and Tests of Fundamental Laws, 1995.

[22] H. Marion *et al.,* Search for variations of fundamental constants using atomic fountain clocks, Phys.Rev.Lett. 90,150801 (2003)

[23] E. Simon, P. Laurent, and A. Clairon, Measurement of the Stark shift of the Cs hyperfine splitting in an atomic fountain, Phys. Rev. A 57, 436 (1998)

[24] W.M. Itano, L.L. Lewis, and D.J. Wineland, Shift of 2S1/2 hyperfine splittings due to blackbody radiation, Phys. Rev. A 25, 35 (1982)

[25] D. Chambon *et al.,* Design and realization of a flywheel oscillator for advanced time and frequency metrology, Rev. Sci. Instrum. 76, 094704 (2005)